Received: 15 May 2019 | Revised: 5 July 2019 | Accepted: 7 July 2019

DOI: 10.1002/dta.2675

RESEARCH ARTICLE

WILEY

Phenethylamine-derived new psychoactive substances 2C-E-FLY, 2C-EF-FLY, and 2C-T-7-FLY: Investigations on their metabolic fate including isoenzyme activities and their toxicological detectability in urine screenings

Lea Wagmann[1] | Nora Hempel[1] | Lilian H.J. Richter[1] | Simon D. Brandt[2] | Alexander Stratford[3] | Markus R. Meyer[1]

[1] Department of Experimental and Clinical Toxicology, Institute of Experimental and Clinical Pharmacology and Toxicology, Center for Molecular Signaling (PZMS), Saarland University, Homburg, Germany

[2] School of Pharmacy and Biomolecular Sciences, Liverpool John Moores University, Liverpool, UK

[3] Synex Synthetics BV, Karveelweg 20, 6222NH, Maastricht, Netherlands

Correspondence
Markus R. Meyer, Department of Experimental and Clinical Toxicology, Institute of Experimental and Clinical Pharmacology and Toxicology, Center for Molecular Signaling (PZMS), Kirrberger Str. Geb. 46, Saarland University, 66421, Homburg, Germany
Email: markus.meyer@uks.eu

Funding information
Armin A. Weber; Hans H. Maurer; Gabriele Ulrich

Abstract

Psychoactive substances of the 2C-series are phenethylamine-based designer drugs that can induce psychostimulant and hallucinogenic effects. The so-called 2C-FLY series contains rigidified methoxy groups integrated in a 2,3,6,7-tetrahydrobenzo[1,2-b:4,5-b']difuran core. The aim of the presented work was to investigate the in vivo and in vitro metabolic fate including isoenzyme activities and toxicological detectability of the three new psychoactive substances (NPS) 2C-E-FLY, 2C-EF-FLY, and 2C-T-7-FLY to allow clinical and forensic toxicologists the identification of these novel compounds. Rat urine, after oral administration, and pooled human liver S9 fraction (pS9) incubations were analyzed by liquid chromatography –high-resolution tandem mass spectrometry (LC–HRMS/MS). By performing activity screenings, the human isoenzymes involved were identified and toxicological detectability in rat urine investigated using standard urine screening approaches (SUSAs) based on gas chromatography (GC)–MS, LC–MS^n, and LC–HRMS/MS. In total, 32 metabolites were tentatively identified. Main metabolic steps consisted of hydroxylation and *N*-acetylation. Phase I metabolic reactions were catalyzed by CYP2D6, 3A4, and FMO3 and *N*-acetylation by NAT1 and NAT2. Methoxyamine was used as a trapping agent for detection of the deaminated metabolite formed by MAO-A and B. Interindividual differences in the metabolism of the 2C-FLY drugs could be caused by polymorphisms of enzymes involved or drug–drug interactions. All three SUSAs were shown to be suitable to detect an intake of these NPS but common metabolites of 2C-E-FLY and 2C-EF-FLY have to be considered during interpretation of analytical findings.

KEYWORDS

drugs of abuse, LC–HRMS/MS, metabolism, new psychoactive substances

1 | INTRODUCTION

Innumerable new psychoactive substances (NPS) are sold as drugs of abuse.[1,2] NPS are often derivatives of drugs under legislative control mimicking their psychoactive effects. This is also true for the 2C-FLY drugs, which are derived from the well-known phenethylamines of the 2C-type and which are also expected to induce psychostimulant and hallucinogenic effects. Chemically, they contain rigidified methoxy groups integrated in a 2,3,6,7-tetrahydrobenzo[1,2-b:4,5-b']difuran core in contrast to the classic 2Cs with two methoxy groups located in positions 2 and 5 of the phenyl ring. Exposure to NPS can result in significant health risks as demonstrated by frequent reports on toxic effects and fatal intoxications.[3-7] Therefore, clinical and forensic toxicologists should be able to reliably detect an intake of NPS. Both parent compounds and metabolites can be suitable screening targets in human biosamples, which are especially important for the development of urine screening approaches.[8] A prerequisite is knowledge of their metabolic fate. Furthermore, knowledge of the isoenzymes involved in the metabolism is important to predict drug–drug/drug–food interactions and/or individual differences found in half-life and excretion patterns.

A series of FLY compounds were originally synthesized to study 5-HT_{2A} receptor function and 2-(4-bromo-2,3,6,7-tetrahydrofuro[2,3-f][1]benzofuran-8-yl)ethanamine (2C-B-FLY) was shown to potently bind to the human 5-HT_{2A} receptor.[9-11] 2C-B-FLY was first reported to the early warning system on NPS implemented by the European Monitoring Centre for Drugs and Drug Addiction (EMCDDA) in 2007 and several times afterwards.[12] However, little is known about the toxicokinetics of 2C-FLY derivatives. Recently, the four 2C-FLY compounds 2C-B-FLY, 2-(4-ethyl-2,3,6,7-tetrahydrofuro[2,3-f][1]benzofuran-8-yl)ethanamine (2C-E-FLY), 2-(4-iodo-2,3,6,7-tetrahydrofuro[2,3-f][1]benzofuran-8-yl)ethanamine (2C-I-FLY), and 2-(4-propylthio-2,3,6,7-tetrahydrofuro[2,3-f][1]benzofuran-8-yl)ethanamine (2C-T-7-FLY) were identified as inhibitors of the monoamine oxidase A.[13] An in vitro metabolism study of 2C-B-FLY was also published recently,[14] but nothing is known about the toxicokinetics of the other 2C-FLY compounds.

Therefore, the aim of the presented work was to close this gap by investigating the in vivo and in vitro metabolic fate of 2C-E-FLY, 2-(4-(2-fluor)ethyl-2,3,6,7-tetrahydrofuro[2,3-f][1]benzofuran-8-yl)ethanamine (2C-EF-FLY), and 2C-T-7-FLY (Figure 1) followed by urinary detectability studies and identification of enzymes involved in initial metabolic steps.

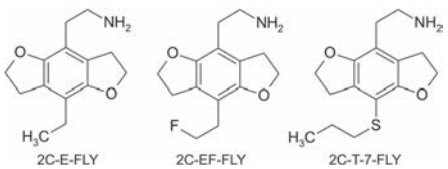

FIGURE 1 Chemical structures of the investigated 2C-FLY drugs

2 | EXPERIMENTAL

2.1 | Chemicals and enzymes

2C-E-FLY, 2C-EF-FLY, and 2C-T-7-FLY were provided as hydrochloride salts by Synex Synthetics BV (Maastricht, Netherlands). Isocitrate, isocitrate dehydrogenase (IDH), superoxide dismutase (SOD), 3′-phosphoadenosine-5′-phosphosulfate (PAPS), *S*-(5′-adenosyl)-L-methionine (SAM), dithiothreitol (DTT), reduced glutathione (GSH), acetylcarnitine transferase (AcT), acetylcarnitine, acetyl coenzyme A (AcCoA), potassium dihydrogenphosphate, dipotassium hydrogenphosphate, Tris base, triethanolamine (TEA), ethylendiaminetetraacetic acid, and methoxyamine were obtained from Sigma-Aldrich (Taufkirchen, Germany) and $NADP^+$ from Biomol (Hamburg, Germany). Acetonitrile (ACN, LC–MS grade), ammonium formate (analytical grade), formic acid (LC–MS grade), methanol (LC–MS grade), and all other chemicals and reagents (analytical grade) were obtained from VWR (Darmstadt, Germany).

The baculovirus-infected insect cell microsomes (Supersomes) containing the human complementary cDNA-expressed cytochrome P450 (CYP) enzymes CYP1A2, CYP2A6, CYP2B6, CYP2C8, CYP2C9, CYP2C19, CYP2D6, CYP3A4 (1 nmol/mL), or CYP2E1, CYP3A5 (2 nmol/mL), or flavin-containing monooxygenase 3 (FMO3), MAO-A, or MAO-B (5 mg protein/mL), or wild type Supersomes without MAO activity as negative control (MAO control, 5 mg protein/mL), and pooled human liver microsomes (pHLMs, 20 mg microsomal protein/mL, 330 pmol total CYP/mg protein), pS9 (20 mg microsomal protein/mL), uridine 5′-diphospho-glucuronosyltransferase (UGT) reaction mixture solution A (25mM UDP-glucuronic acid), and UGT reaction mixture solution B (250mM Tris–HCl, 40mM $MgCl_2$, and 0.125 mg/mL alamethicin) were obtained from Corning (Amsterdam, Netherlands). Supersomes containing human complementary cDNA-expressed NAT1 (arylamine NAT1*4, wild-type allele) and NAT2 (arylamine NAT2*4 wild-type allele) were obtained from BD Biosciences (Heidelberg, Germany). After delivery, the enzyme preparations and PAPS were thawed at 37°C, aliquoted, snap-frozen in liquid nitrogen, and stored at −80°C until use.

2.2 | Rat urine samples

As already described in previous studies, the in vivo experiments were performed using urine samples from male Wistar rats (Charles River, Sulzfeld, Germany) for toxicological diagnostic reasons according to German law ("Tierschutzgesetz", Bundesministerium der Justiz und für Verbraucherschutz, 2018, dealing with the treatment of laboratory animals and the experimental design aiming to prevent unnecessary pain, harm, and distress).[15-17] First, blank urines were collected over a period of 24 hours to verify the absence of interfering compounds. Afterwards the compounds were administered in an aqueous solution via gastric intubation as a single dose of 0.2 mg/kg body weight (BW) for toxicological detectability studies (low dose) and a single dose of 2 mg/kg BW (high dose) for identification of the metabolites and toxicological detectability studies. During the collection of urine over a

period of 24 hours, the rats were housed in metabolism cages and urine was collected separated from feces. The urine samples were analyzed directly and remaining samples were aliquoted and stored at −20°C. One rat was used per NPS.

2.3 | Rat urine sample preparation for identification of metabolites

2.3.1 | Precipitation

Identification of phase I and II metabolites in rat urine was performed after urine precipitation (UP) as described elsewhere.[18] A volume of 100 µL urine collected after high dose administration was precipitated with 500 µL acetonitrile. The mixture was vortexed and centrifuged for 2 minutes at 18 407 x g. The supernatant was evaporated to dryness under a stream of nitrogen. The residue was reconstituted in 50 µL of a 1:1 (v/v) mixture of eluents A and B and transferred to an autosampler vial. One µL was injected onto the LC−HRMS/MS system.

2.3.2 | Solid-phase extraction

According to Maurer et al,[19] 2.5 mL of high dose rat urine was poured into a centrifugal glass and 2 mL of distilled water and 50 µL of 0.01 mg/mL trimipramine-d_3 as internal standard were added. The HCX cartridge was conditioned with 1 mL methanol and 1 mL distilled water before transferring the samples to the cartridge. After the passage of the sample, the cartridge was washed with 1 mL distilled water, 1 mL 0.01 M hydrochloric acid, and 2 mL methanol. Thereafter, compounds of interest were eluted with 1 mL of a mixture of methanol/aqueous ammonia 33% (98:2, v/v) into an autosampler vial and evaporated to dryness under a stream of nitrogen at 60°C. The extract was reconstituted in 50 µL methanol and 1 µL was injected onto the LC-HRMS/MS system.

2.4 | pS9 incubations

As described before,[20] the final incubation volume was 150 µL and the final protein concentration was 2 mg/mL. All given concentrations are final concentrations in the incubation mixture. First, a mixture containing 25 µg/mL alamethicin (UGT reaction mixture solution B), 90mM phosphate buffer (pH 7.4), 2.5mM Mg^{2+}, 2.5mM isocitrate, 0.6mM $NADP^+$, 0.8 U/mL IDH, 100 U/mL SOD, 0.1mM AcCoA, 2.3mM acetyl carnitine, 8 U/mL AcT, and 2 mg/mL pS9 was preincubated for 10 minutes at 37°C. Afterwards, 2.5mM UDP glucuronic acid (UGT reaction mix solution A), 40 µM aqueous PAPS, 1.2mM SAM, 1mM DTT, and 10mM GSH were added. The reactions were started by addition of 25 µM of one of the 2C-FLY derivatives in phosphate buffer and the tube was incubated for 6 hours. After 1 hour, 60 µL of the incubation mixture was transferred into another tube and the reaction was terminated by addition of 20 µL ice-cold acetonitrile. The remaining mixture (90 µL) was incubated for an additional 5 hours and then stopped with 30 µL ice-cold acetonitrile. All solutions were cooled for 30 minutes at −20°C, centrifuged for 2 minutes at 18 407 x g, and 50 µL of the supernatants were transferred to autosampler vials. One µL was injected onto the LC−HRMS/MS system. Blank incubations without 2C-FLY derivative and control samples without pS9 were prepared to confirm the absence of interfering compounds and to identify compounds that are not of metabolic origin. All incubations were done in duplicate.

2.5 | Isoenzyme activity screenings

2.5.1 | Monooxygenases activity screening

The microsomal incubations were performed at 37°C for 30 minutes with 25 µM of the 2C-FLY analog and 50 pmol/mL CYP isoenzyme (CYP1A2, 2A6, 2B6, 2C8, 2C9, 2C19, 2D6, 2E1, 3A4, or 3A5) or 0.25 mg protein/mL FMO3.[21] The incubation mixtures with a final volume of 50 µL also contained 90mM phosphate buffer (pH 7.4), the $NADP^+$ regenerating system (1.2mM $NADP^+$, 5mM Mg^{2+}, 5mM isocitrate, 0.5 U/mL IDH), and 200 U/mL SOD. All incubations were performed with phosphate buffer except for the ones with CYP2A6 and CYP2C9 which were performed with 90mM Tris buffer (pH 7.4). A positive control with 1 mg protein/mL pHLM and a blank incubation without enzyme was also performed. The reactions were started by addition of the $NADP^+$ regenerating system and terminated by addition of 50 µL of ice-cold acetonitrile. Afterwards the mixture was centrifuged for 5 minutes at 18,407 x g and 50 µL of the supernatant were transferred to an autosampler vial. One µL was injected onto the LC−HRMS/MS system. All given concentrations are final concentrations.

2.5.2 | Monoamine oxidases activity screening

The incubations were performed at 37°C for 2 hours at a final incubation volume of 150 µL containing 25 µM of the 2C-FLY analog, MAO-A or MAO-B (0.2 mg protein/mL), 90mM phosphate buffer, and 10mM of the aldehyde trapping agent methoxyamine.[14] All given concentrations were final concentrations and a negative control with MAO control was also performed. The reactions were started by addition of the enzyme and terminated with 150 µL ice-cold acetonitrile. Afterwards, the mixture was centrifuged for 2 minutes at 18 407 x g and the supernatant was transferred to an autosampler vial. Five µL were injected onto the hydrophilic interaction liquid chromatography (HILIC)−HRMS/MS system.

2.5.3 | *N*-Acetyltransferases activity screening

Incubations were performed at 37°C for 30 minutes with 50 µM of substrate and NAT1 or NAT2 (0.05 mg protein/mL).[22,23] Besides substrate and enzyme, the incubation mixture with final volume of 150 µL also contained buffer at pH 7.5 consisting of 100mM TEA, 500mM ethylendiaminetetraacetic acid, and 50mM DTT, and the CoA-system consisting of 0.1mM AcCoA, 2.3mM acetylcarnitine, and 0.008 U/µL AcT. First, the incubation mixture was preincubated at 37°C for 10 minutes. Subsequently, the reactions were started by addition of substrate and terminated after 30 minutes by addition of 50 µL of

TABLE 1 2C-E-FLY, 2C-EF-FLY, 2C-T-7-FLY, and their phase I and II metabolites identified in rat urine and/or in vitro incubations by means of LC−HRMS/MS together with their identification numbers (iDs), metabolic reactions, precursor ion masses (PMs) recorded in MS^1, characteristic fragment ions (FIs) in MS^2, relative intensities in MS^2, calculated exact masses, elemental compositions, deviations of the measured from the calculated masses, and retention times (RTs)

Metabolite iD	Metabolic Reaction	Characteristic ions at Measured Accurate Masses, m/z	Relative Intensity in MS^2, %	Calculated Exact Masses, m/z	Elemental Composition	Error, ppm	RT, min
2C-E-FLY	Parent compound	PM at m/z 234.1486	8	234.1488	$C_{14}H_{20}O_2N$	−0.76	4.60
		FI at m/z 217.1225	100	217.1222	$C_{14}H_{17}O_2$	1.24	
		FI at m/z 188.0831	13	188.0831	$C_{12}H_{12}O_2$	0.00	
		FI at m/z 161.0594	2	161.0596	$C_{10}H_9O_2$	−1.42	
		FI at m/z 133.0650	1	133.0647	C_9H_9O	2.14	
M1	Hydroxylation	PM at m/z 250.1433	25	250.1437	$C_{14}H_{20}O_3N$	−1.57	3.36
		FI at m/z 233.1170	100	233.1171	$C_{14}H_{17}O_3$	−0.62	
		FI at m/z 215.1063	26	215.1066	$C_{14}H_{15}O_2$	−1.30	
		FI at m/z 190.0986	61	190.0988	$C_{12}H_{14}O_2$	−0.81	
		FI at m/z 175.0751	8	175.0753	$C_{11}H_{11}O_2$	−1.03	
M2	Hydroxylation	PM at m/z 250.1435	10	250.1437	$C_{14}H_{20}O_3N$	−0.77	3.74
		FI at m/z 233.1171	64	233.1171	$C_{14}H_{17}O_3$	0.00	
		FI at m/z 215.1065	100	215.1066	$C_{14}H_{15}O_2$	−0.37	
		FI at m/z 203.1065	10	203.1066	$C_{13}H_{15}O_2$	−0.39	
		FI at m/z 187.1115	42	187.1117	$C_{13}H_{15}O$	−0.88	
		FI at m/z 159.0802	14	159.0804	$C_{11}H_{11}O$	−1.04	
		FI at m/z 131.0491	1	131.0491	C_9H_7O	0.00	
M3	Dihydroxylation	PM at m/z 266.1392	32	266.1386	$C_{14}H_{20}O_4N$	2.22	2.13
		FI at m/z 249.1118	100	249.1121	$C_{14}H_{17}O_4$	−1.04	
		FI at m/z 218.0934	17	218.0937	$C_{13}H_{14}O_3$	−1.23	
		FI at m/z 203.1064	27	203.1066	$C_{13}H_{15}O_2$	−0.88	
		FI at m/z 190.0985	18	190.0988	$C_{12}H_{14}O_2$	−1.34	
		FI at m/z 175.0752	6	175.0753	$C_{11}H_{11}O_2$	−0.45	
M4	Dihydroxylation	PM at m/z 266.1386	7	266.1386	$C_{14}H_{20}O_4N$	0.00	2.93
		FI at m/z 248.1276	24	248.1280	$C_{14}H_{18}O_3N$	−1.79	
		FI at m/z 230.1172	12	230.1175	$C_{14}H_{16}O_2N$	−1.21	
		FI at m/z 201.0910	100	201.0909	$C_{13}H_{13}O_2$	0.35	
		FI at m/z 191.1069	1	191.1066	$C_{12}H_{15}O_2$	1.68	
		FI at m/z 188.0830	5	188.0831	$C_{12}H_{12}O_2$	−0.56	
		FI at m/z 173.0959	5	173.0960	$C_{12}H_{13}O$	−0.66	
		FI at m/z 131.0490	1	131.0491	C_9H_7O	−0.76	
M5	Dihydroxylation	PM at m/z 266.1381	22	266.1386	$C_{14}H_{20}O_4N$	−1.91	3.16
		FI at m/z 248.1275	36	248.1280	$C_{14}H_{18}O_3N$	−2.19	
		FI at m/z 231.1011	100	231.1015	$C_{14}H_{15}O_3$	−1.71	
		FI at m/z 213.0905	46	213.0909	$C_{14}H_{13}O_2$	−2.02	
		FI at m/z 203.1062	18	203.1066	$C_{13}H_{15}O_2$	−1.87	
		FI at m/z 185.0959	16	185.0960	$C_{13}H_{13}O$	−0.62	
		FI at m/z 157.0646	4	157.0647	$C_{11}H_9O$	−0.73	
		FI at m/z 131.0500	1	131.0491	C_9H_7O	6.87	
M6	Dihydroxylation	PM at m/z 266.1396	23	266.1386	$C_{14}H_{20}O_4N$	3.73	3.78
		FI at m/z 249.1119	23	249.1121	$C_{14}H_{17}O_4$	−0.64	
		FI at m/z 231.1015	29	231.1015	$C_{14}H_{15}O_3$	0.00	
		FI at m/z 203.1066	100	203.1066	$C_{13}H_{15}O_2$	0.00	
		FI at m/z 188.0830	3	188.0831	$C_{12}H_{12}O_2$	−0.56	
		FI at m/z 175.0752	13	175.0753	$C_{11}H_{11}O_2$	−0.45	
M7	Trihydroxylation	PM at m/z 282.1336	100	282.1335	$C_{14}H_{20}O_5N$	0.27	2.72
		FI at m/z 265.1067	57	265.1070	$C_{14}H_{17}O_5$	−1.03	
		FI at m/z 247.0962	13	247.0964	$C_{14}H_{15}O_4$	−0.85	
		FI at m/z 229.0861	97	229.0858	$C_{14}H_{13}O_3$	1.12	

(Continues)

TABLE 1 (Continued)

Metabolite iD	Metabolic Reaction	Characteristic ions at Measured Accurate Masses, m/z	Relative Intensity in MS^2, %	Calculated Exact Masses, m/z	Elemental Composition	Error, ppm	RT, min
		FI at m/z 219.1013	64	219.1015	$C_{13}H_{15}O_3$	−0.89	
		FI at m/z 203.1063	31	203.1066	$C_{13}H_{15}O_2$	−1.38	
		FI at m/z 175.0753		175.0753	$C_{11}H_{11}O_2$	0.00	
M8	Carboxylation	PM at m/z 264.1231	18	264.1230	$C_{14}H_{18}O_4N$	0.92	3.43
		FI at m/z 247.0966	100	247.0964	$C_{14}H_{15}O_4$	0.77	
		FI at m/z 229.0858	1	229.0858	$C_{14}H_{13}O_3$	0.00	
		FI at m/z 201.0908	63	201.0909	$C_{13}H_{13}O_2$	−0.64	
		FI at m/z 188.0829	2	188.0831	$C_{12}H_{12}O_2$	−1.09	
		FI at m/z 173.0959	8	173.0960	$C_{12}H_{13}O$	−0.66	
M9	Hydroxylation + *O*-glucuronidation	PM at m/z 426.1757	16	426.1758	$C_{20}H_{28}O_9N$	−0.19	3.32
		FI at m/z 250.1434	71	250.1437	$C_{14}H_{20}O_3N$	−1.17	
		FI at m/z 233.1170	100	233.1171	$C_{14}H_{17}O_3$	−0.62	
		FI at m/z 215.1064	20	215.1066	$C_{14}H_{15}O_2$	−0.84	
		FI at m/z 187.1115	3	187.1117	$C_{13}H_{15}O$	−0.88	
		FI at m/z 159.0803	1	159.0804	$C_{11}H_{11}O$	−0.41	
M10	*N*-acetylation	PM at m/z 276.1594	35	276.1593	$C_{16}H_{22}O_3N$	0.20	6.21
		FI at m/z 234.1486	5	234.1488	$C_{14}H_{20}O_2N$	−0.76	
		FI at m/z 217.1222	100	217.1222	$C_{14}H_{17}O_2$	0.00	
		FI at m/z 188.0830	16	188.0831	$C_{12}H_{12}O_2$	−0.56	
		FI at m/z 161.0596	3	161.0596	$C_{10}H_9O_2$	0.00	
M11	*N*-acetylation + hydroxylation	PM at m/z 292.1542	92	292.1543	$C_{16}H_{22}O_4N$	−0.20	4.65
		FI at m/z 274.1435	12	274.1437	$C_{16}H_{20}O_3N$	−0.71	
		FI at m/z 250.1437	16	250.1437	$C_{14}H_{20}O_3N$	0.00	
		FI at m/z 233.1172	100	233.1171	$C_{14}H_{17}O_3$	0.24	
		FI at m/z 215.1066	93	215.1066	$C_{14}H_{15}O_2$	0.00	
		FI at m/z 203.1068	11	203.1066	$C_{13}H_{15}O_2$	1.08	
		FI at m/z 187.1115	9	187.1117	$C_{13}H_{15}O$	−0.88	
		FI at m/z 159.0804	5	159.0804	$C_{11}H_{11}O$	0.00	
M12	*N*-acetylation + dihydroxylation	PM at m/z 308.1501	27	308.1492	$C_{16}H_{22}O_5N$	3.01	4.63
		FI at m/z 290.1385	82	290.1386	$C_{16}H_{20}O_4N$	−0.37	
		FI at m/z 272.1279	1	272.1280	$C_{14}H_{20}O_3N$	−0.53	
		FI at m/z 248.1278	100	248.1280	$C_{14}H_{18}O_3N$	−0.98	
		FI at m/z 231.1012	80	231.1015	$C_{14}H_{15}O_3$	−1.27	
		FI at m/z 213.0908	1	213.0909	$C_{14}H_{13}O_2$	−0.61	
		FI at m/z 203.1065	12	203.1066	$C_{13}H_{15}O_2$	−0.39	
		FI at m/z 185.0960	1	185.0960	$C_{13}H_{13}O$	0.00	
M13	Methoxyamine adduct	PM at m/z 262.1437	7	262.1437	$C_{15}H_{20}O_3N$	0.00	1.21
		FI at m/z 203.1068	100	203.1066	$C_{13}H_{15}O_2$	1.08	
		FI at m/z 190.0987	30	190.0988	$C_{12}H_{14}O_2$	−0.29	
		FI at m/z 175.0754	7	175.0753	$C_{11}H_{11}O_2$	0.69	
2C-EF-FLY	Parent compound	PM at m/z 252.1394	15	252.1394	$C_{14}H_{19}O_2NF$	0.00	4.44
		FI at m/z 235.1129	100	235.1128	$C_{14}H_{16}O_2F$	0.39	
		FI at m/z 207.0815	5	207.0815	$C_{12}H_{12}O_2F$	0.00	
		FI at m/z 188.0831	5	188.0831	$C_{12}H_{12}O_2$	0.00	
		FI at m/z 159.0805	3	159.0804	$C_{11}H_{11}O$	0.85	
		FI at m/z 131.0856	1	131.0855	$C_{10}H_{11}$	1.14	
M1	Oxidative defluorination	PM at m/z 250.1433	25	250.1437	$C_{14}H_{20}O_3N$	−1.57	3.36
		FI at m/z 233.1170	100	233.1171	$C_{14}H_{17}O_3$	−0.62	
		FI at m/z 215.1063	26	215.1066	$C_{14}H_{15}O_2$	−1.30	
		FI at m/z 190.0986	61	190.0988	$C_{12}H_{14}O_2$	−0.81	
		FI at m/z 175.0751	8	175.0753	$C_{11}H_{11}O_2$	−1.03	
M14	Hydroxylation	PM at m/z 268.1340	39	268.1343	$C_{14}H_{19}O_3NF$	−1.01	3.21

(Continues)

TABLE 1 (Continued)

Metabolite iD	Metabolic Reaction	Characteristic ions at Measured Accurate Masses, m/z	Relative Intensity in MS^2, %	Calculated Exact Masses, m/z	Elemental Composition	Error, ppm	RT, min
		FI at m/z 251.1074	100	251.1077	$C_{14}H_{16}O_3F$	−1.28	
		FI at m/z 233.0969	1	233.0972	$C_{14}H_{14}O_2F$	−1.11	
		FI at m/z 213.0907	2	213.0909	$C_{14}H_{13}O_2$	−1.08	
		FI at m/z 190.0985	18	190.0988	$C_{12}H_{14}O_2$	−1.34	
M15	Hydroxylation	PM at m/z 268.1339	1	268.1343	$C_{14}H_{19}O_3NF$	−1.39	3.38
		FI at m/z 250.1234	46	250.1237	$C_{14}H_{17}O_2NF$	−1.23	
		FI at m/z 233.0968	100	233.0972	$C_{14}H_{14}O_2F$	−1.54	
		FI at m/z 221.0969	11	221.0972	$C_{13}H_{14}O_2F$	−1.17	
		FI at m/z 205.1021	21	205.1022	$C_{13}H_{14}OF$	−0.70	
		FI at m/z 185.0958	8	185.0960	$C_{13}H_{13}O$	−1.16	
		FI at m/z 158.0723	4	158.0725	$C_{11}H_{10}O$	−1.52	
M16	Dihydroxylation	PM at m/z 284.1287	22	284.1292	$C_{14}H_{19}O_4NF$	−1.71	2.75
		FI at m/z 266.1181	68	266.1186	$C_{14}H_{17}O_3NF$	−1.96	
		FI at m/z 248.1079	100	248.1081	$C_{14}H_{15}O_2NF$	−0.63	
		FI at m/z 231.0811	62	231.0815	$C_{14}H_{12}O_2F$	−1.76	
		FI at m/z 217.0856	39	217.0858	$C_{13}H_{13}O_3$	−1.13	
		FI at m/z 199.0753	29	199.0753	$C_{13}H_{11}O_2$	0.00	
		FI at m/z 189.0910	1	189.0909	$C_{12}H_{13}O_2$	0.37	
		FI at m/z 183.0804	8	183.0804	$C_{13}H_{11}O$	0.00	
M17	Dihydroxylation	PM at m/z 284.1290	48	284.1292	$C_{14}H_{19}O_4NF$	−0.66	3.13
		FI at m/z 266.1183	12	266.1186	$C_{14}H_{17}O_3NF$	−1.21	
		FI at m/z 249.0917	65	249.0921	$C_{14}H_{14}O_3F$	−1.50	
		FI at m/z 231.0816	50	231.0815	$C_{14}H_{12}O_2F$	0.40	
		FI at m/z 221.0970	100	221.0972	$C_{13}H_{14}O_2F$	−0.71	
		FI at m/z 203.0864	39	203.0866	$C_{13}H_{12}OF$	−0.95	
M8	Oxidative defluorination + oxidation to carboxylic acid	PM at m/z 264.1228	21	264.1230	$C_{14}H_{18}O_4N$	−0.60	3.43
		FI at m/z 247.0966	100	247.0964	$C_{14}H_{15}O_4$	0.77	
		FI at m/z 229.0856	2	229.0858	$C_{14}H_{13}O_3$	−1.07	
		FI at m/z 201.0907	65	201.0909	$C_{13}H_{13}O_2$	−1.14	
		FI at m/z 173.0959	8	173.0960	$C_{12}H_{13}O$	−0.66	
		FI at m/z 145.1010	2	145.1011	$C_{11}H_{13}$	−0.69	
M18	*N*-acetylation	PM at m/z 294.1495	51	294.1499	$C_{16}H_{21}O_3NF$	−1.43	5.79
		FI at m/z 252.1394	14	252.1394	$C_{14}H_{19}O_2NF$	0.00	
		FI at m/z 235.1128	100	235.1128	$C_{14}H_{16}O_2F$	0.00	
		FI at m/z 207.0815	6	207.0815	$C_{12}H_{12}O_2F$	0.00	
		FI at m/z 188.0830	8	188.0831	$C_{12}H_{12}O_2$	−0.56	
		FI at m/z 159.0804	4	159.0804	$C_{11}H_{11}O$	0.00	
M19	Methoxyamine adduct	PM at m/z 280.1336	9	280.1343	$C_{15}H_{19}O_3NF$	−0.61	1.23
		FI at m/z 221.0972	100	221.0972	$C_{13}H_{14}O_2F$	0.00	
		FI at m/z 208.0894	19	208.0893	$C_{12}H_{13}O_2F$	0.32	
		FI at m/z 188.0831	1	188.0831	$C_{12}H_{12}O_2$	0.00	
2C-T-7-FLY	Parent compound	PM at m/z 280.1359	10	280.1365	$C_{15}H_{22}O_2NS$	−2.14	5.29
		FI at m/z 263.1095	100	263.1099	$C_{15}H_{19}O_2S$	−1.71	
		FI at m/z 221.0627	26	221.0630	$C_{12}H_{13}O_2S$	−1.36	
		FI at m/z 188.0827	12	188.0831	$C_{12}H_{12}O_2$	−2.15	
		FI at m/z 159.0801	2	159.0804	$C_{11}H_{11}O$	−1.67	
		FI at m/z 131.0854	1	131.0855	$C_{10}H_{11}$	−0.38	
M20	Oxidation to sulfoxide	PM at m/z 296.1309	88	296.1314	$C_{15}H_{22}O_3NS$	−1.06	3.80
		FI at m/z 279.1041	14	279.1049	$C_{15}H_{19}O_3S$	−2.74	
		FI at m/z 237.0575	100	237.0579	$C_{12}H_{13}O_3S$	−1.33	

(Continues)

TABLE 1 (Continued)

Metabolite iD	Metabolic Reaction	Characteristic ions at Measured Accurate Masses, m/z	Relative Intensity in MS^2, %	Calculated Exact Masses, m/z	Elemental Composition	Error, ppm	RT, min
		FI at m/z 223.0421	1	223.0423	$C_{11}H_{11}O_3S$	−0.74	
		FI at m/z 219.0471	24	219.0473	$C_{12}H_{11}O_2S$	−1.14	
		FI at m/z 205.0856	35	205.0858	$C_{12}H_{13}O_3$	−1.19	
		FI at m/z 159.0803	1	159.0804	$C_{11}H_{11}O$	4.62	
		FI at m/z 131.0853	1	131.0855	$C_{10}H_{11}$	−1.15	
M21	Hydroxylation	PM at m/z 296.1310	4	296.1314	$C_{15}H_{22}O_3NS$	−1.40	3.98
		FI at m/z 279.1047	100	279.1049	$C_{15}H_{19}O_3S$	−0.59	
		FI at m/z 261.0941	1	261.0943	$C_{15}H_{17}O_2S$	−0.77	
		FI at m/z 221.0628	33	221.0630	$C_{12}H_{13}O_2S$	−0.90	
		FI at m/z 188.0830	10	188.0831	$C_{12}H_{12}O_2$	−0.56	
		FI at m/z 159.0802	2	159.0804	$C_{11}H_{11}O$	−1.04	
		FI at m/z 131.0854	1	131.0855	$C_{10}H_{11}$	−0.38	
M22	Oxidation to sulfone	PM at m/z 312.1262	70	312.1263	$C_{15}H_{22}O_4NS$	−0.73	2.83
		FI at m/z 295.0993	9	295.0998	$C_{15}H_{19}O_4S$	−1.62	
		FI at m/z 237.0575	12	237.0579	$C_{12}H_{13}O_3S$	−1.75	
		FI at m/z 223.0422	100	223.0423	$C_{11}H_{11}O_3S$	−0.29	
		FI at m/z 219.0472	9	219.0473	$C_{12}H_{11}O_2S$	−0.68	
		FI at m/z 205.0857	33	205.0858	$C_{12}H_{13}O_3$	−0.70	
		FI at m/z 188.0830	3	188.0831	$C_{12}H_{12}O_2$	−0.56	
		FI at m/z 176.0831	27	176.0831	$C_{11}H_{12}O_2$	0.00	
		FI at m/z 159.0803	2	159.0804	$C_{11}H_{11}O$	−0.41	
M23	Dihydroxylation	PM at m/z 312.1261	63	312.1263	$C_{15}H_{22}O_4NS$	−0.73	3.91
		FI at m/z 295.0995	100	295.0998	$C_{15}H_{19}O_4S$	−0.95	
		FI at m/z 253.0526	22	253.0528	$C_{12}H_{13}O_4S$	−0.90	
		FI at m/z 235.0421	11	235.0423	$C_{12}H_{11}O_3S$	−0.70	
		FI at m/z 218.0393	25	218.0395	$C_{12}H_{10}O_2S$	−1.03	
		FI at m/z 207.0473	63	207.0473	$C_{11}H_{11}O_2S$	0.00	
		FI at m/z 188.0829	1	188.0831	$C_{12}H_{12}O_2$	−1.09	
		FI at m/z 174.0674	38	174.0675	$C_{11}H_{10}O_2$	−0.31	
M24	Carboxylation	PM at m/z 310.1104	42	310.1107	$C_{15}H_{20}O_4NS$	−0.90	4.00
		FI at m/z 293.0840	100	293.0841	$C_{15}H_{17}O_4S$	−0.44	
		FI at m/z 275.0731	1	275.0736	$C_{15}H_{15}O_2S$	−1.69	
		FI at m/z 220.0548	13	220.0552	$C_{12}H_{12}O_2S$	−1.70	
		FI at m/z 188.0829	38	188.0831	$C_{12}H_{12}O_2$	−1.09	
		FI at m/z 159.0802	4	159.0804	$C_{11}H_{11}O$	−1.04	
		FI at m/z 131.0853	1	131.0855	$C_{10}H_{11}$	−1.15	
M25	*S*-Dealkylation	PM at m/z 238.0889	1	238.0895	$C_{12}H_{16}O_2NS$	−2.72	4.17
		FI at m/z 221.0628	100	221.0630	$C_{12}H_{13}O_2S$	−0.90	
		FI at m/z 188.0830	11	188.0831	$C_{12}H_{12}O_2$	−0.56	
		FI at m/z 159.0804	1	159.0804	$C_{11}H_{11}O$	0.00	
M26	*N*-acetylation	PM at m/z 322.1463	42	322.1471	$C_{17}H_{24}O_3NS$	−2.37	6.85
		FI at m/z 280.1358	4	280.1365	$C_{15}H_{22}O_2S$	−2.49	
		FI at m/z 263.1095	70	263.1099	$C_{15}H_{19}O_2S$	−1.71	
		FI at m/z 247.1198	89	247.1202	$C_{14}H_{17}O_3S$	−1.69	
		FI at m/z 221.0625	26	221.0630	$C_{12}H_{13}O_2S$	−2.26	
		FI at m/z 188.0828	100	188.0831	$C_{12}H_{12}O_2$	−1.62	
		FI at m/z 159.0798	2	159.0804	$C_{11}H_{11}O$	−3.55	
		FI at m/z 131.0853	1	131.0855	$C_{10}H_{11}$	−1.15	
M27	*N*-acetylation + oxidation to sulfoxide	PM at m/z 338.1411	100	338.1420	$C_{17}H_{24}O_4NS$	−2.60	5.21
		FI at m/z 296.1306	6	296.1314	$C_{15}H_{22}O_3NS$	−2.75	
		FI at m/z 279.1042	5	279.1049	$C_{15}H_{19}O_3S$	−2.38	
		FI at m/z 236.0496	35	236.0501	$C_{12}H_{12}O_3S$	−2.07	
		FI at m/z 219.0467	48	219.0473	$C_{12}H_{11}O_2S$	−2.97	

(Continues)

TABLE 1 (Continued)

Metabolite iD	Metabolic Reaction	Characteristic ions at Measured Accurate Masses, m/z	Relative Intensity in MS^2, %	Calculated Exact Masses, m/z	Elemental Composition	Error, ppm	RT, min
		FI at m/z 205.0855	2	205.0858	$C_{11}H_{13}O_3$	−1.68	
		FI at m/z 188.0827	12	188.0831	$C_{12}H_{12}O_2$	−2.15	
M28	*N*-acetylation + oxidation to sulfone	PM at m/z 354.1360	41	354.1369	$C_{17}H_{24}O_5NS$	−2.52	4.16
		FI at m/z 294.0787	20	294.0794	$C_{14}H_{16}O_4NS$	−2.31	
		FI at m/z 276.0681	1	276.0688	$C_{14}H_{14}O_3NS$	−2.58	
		FI at m/z 247.1199	28	247.1202	$C_{14}H_{17}O_3N$	−1.29	
		FI at m/z 235.0418	100	235.0423	$C_{12}H_{11}O_3S$	−1.97	
		FI at m/z 219.0468	13	219.0473	$C_{12}H_{11}O_2S$	−2.51	
		FI at m/z 217.0314	26	217.0317	$C_{12}H_9O_2S$	−1.38	
		FI at m/z 205.0313	3	205.0317	$C_{11}H_9O_2S$	−1.95	
		FI at m/z 188.0829	34	188.0831	$C_{12}H_{12}O_2$	−1.09	
		FI at m/z 186.0671	20	186.0675	$C_{12}H_{10}O_2$	−1.91	
M29	*N*-acetylation + carboxylation	PM at m/z 352.1200	39	352.1212	$C_{17}H_{22}O_5NS$	−3.53	5.34
		FI at m/z 334.1095	100	334.1107	$C_{17}H_{20}O_4NS$	−3.53	
		FI at m/z 310.1094	1	310.1107	$C_{15}H_{20}O_4NS$	−4.12	
		FI at m/z 293.0830	22	293.0841	$C_{15}H_{17}O_4S$	−3.85	
		FI at m/z 275.0728	25	275.0736	$C_{15}H_{15}O_3S$	−2.42	
		FI at m/z 247.1194	32	247.1202	$C_{14}H_{17}O_3N$	−3.31	
		FI at m/z 233.0624	13	233.0630	$C_{13}H_{13}O_2S$	−2.57	
		FI at m/z 219.0470	56	219.0473	$C_{12}H_{11}O_2S$	−1.60	
		FI at m/z 188.0826	94	188.0831	$C_{12}H_{12}O_2$	−2.68	
M30	Methoxyamine adduct	PM at m/z 308.1311	10	308.1314	$C_{16}H_{22}O_3NS$	−1.02	1.19
		FI at m/z 249.0944	100	249.0943	$C_{14}H_{17}O_2S$	0.40	
		FI at m/z 236.0862	30	236.0865	$C_{13}H_{16}O_2S$	−1.16	
		FI at m/z 207.0473	29	207.0473	$C_{11}H_{11}O_2S$	0.00	

ice-cold acetonitrile. The mixture was centrifuged for 5 minutes at 18 407 x g and 50 µL of the supernatant was transferred to an autosampler vial. One µL was injected onto the LC–HRMS/MS system.

2.6 | LC–HRMS/MS conditions

Analyses were performed using a Thermo Fisher scientific (TF, Dreieich, Germany) Dionex UltiMate 3000 Rapid Separation (RS) UHPLC system with a quaternary UltiMate 3000 RS pump and an UltiMate 3000 RS autosampler controlled by the TF Chromeleon software version 6.80. It was coupled to a TF Q-Exactive Plus, equipped with a heated electrospray ionization II source (HESI II). The mass spectrometer was mass calibrated before analysis using a Positive Mode Cal Mix (Supelco, Bellefonte, PA, USA).

For all measurements except the MAO activity screening, the LC conditions were as follows: TF Accucore PhenylHexyl column (100 mm x 2.1 mm inside diameter, ID, 2.6 µm particle size); gradient elution with eluent A (2mM aqueous ammonium formate solution containing 0.1% (v/v) formic acid) and eluent B (ammonium formate solution with acetonitrile/methanol (50:50, v/v) containing 0.1% (v/v) formic acid and 1% (v/v) water). The gradient was set as follows: 0–1 minute 1% B, 1–10 minutes to 99% B, 10–11.5 minutes hold 99% B, 11.5–13.5 minutes hold 1% B. The flow rate settings were as follows: 0–11.5 minutes at 0.500 mL/min, and 11.5–13.5 minutes at 0.800 mL/min.[24]

Conditions for the MAO activity screenings were as follows: Macherey-Nagel (Düren, Germany) HILIC Nucleodur column (125 mm x 3 mm ID, 3 µm particle size). As mobile phases eluent C (200mM aqueous ammonium acetate) and eluent D (acetonitrile containing 0.1%, v/v, formic acid) were used. The gradient was set as follows: 0–8.5 minutes 98% D to 40% D, 8.5–10 minutes hold 40% D, 10–12 min hold 98% D. The flow rate was set to 0.500 mL/min.

The HESI-II conditions were as follows: Heater temperature, 320°C; ion transfer capillary temperature, 320°C; sheath gas, 60 arbitrary units (AU); auxiliary gas, 10 AU; spray voltage, 4.00 kV, positive mode; S-lens RF level, 50.0. Mass spectrometry was performed in positive electrospray ionization (ESI) full-scan mode and targeted MS^2 mode with an inclusion list containing masses of expected metabolites. The settings for full-scan data acquisition were chosen as follows: resolution, 35 000; automatic gain control (AGC) target, 1e6; maximum injection time (IT), 120 ms; scan range, m/z 200–1200 (2C-E-FLY), m/z 200–1100 (2C-EF-FLY), or m/z 200–800 (2C-T-7-FLY). The settings for the targeted MS^2 mode were chosen as follows: resolution, 17,500; AGC target, 2e5; maximum IT, 250 ms; isolation window, m/z 1.0; stepped normalized collision energy (NCE) with steps 17.5%, 35%, 52.5%; pick others, enabled. For data evaluation, TF Xcalibur Qual Browser software version 2.2 SP 1.48 was used.

2.7 | Toxicological detectability in rat urine

Standard urine screening approaches (SUSAs) by gas chromatography (GC)-MS, LC-ion trap (IT)-MS, and LC-HRMS/MS were performed as described before.[16,18,19,24] Briefly, urine precipitation with acetonitrile was performed for the LC-based SUSAs and liquid–liquid extraction (LLE) after acidic hydrolysis followed by acetylation for the GC–MS SUSA.

3 | RESULTS AND DISCUSSION

3.1 | Identification of metabolites

For identification of metabolites, MS^1 data after analysis of the in vivo and in vitro samples were screened for exact precursor masses (PMs) of expected metabolites. A maximum deviation of 5 ppm between measured and calculated exact PM was accepted. Afterwards, the

TABLE 2 Absolute peak areas of 2C-E-FLY, 2C-EF-FLY, 2C-T-7-FLY, and their phase I and II metabolites in MS^1 derived from analyses of rat urine samples after urine precipitation (UP) or solid-phase extraction (SPE) or pS9 incubations by LC–HRMS/MS. metabolite iDs correspond to Table 1. -, not detected

Metabolite iD	Metabolic Reaction	Calculated Exact Masses, *m/z*	Rat		pS9	
			UP	SPE	1 h	6 h
2C-E-FLY	Parent compound	234.1488	2.35E+07	5.23E+08	1.11E+09	1.27E+09
M1	Hydroxylation	250.1437	1.23E+08	1.39E+09	-	-
M2	Hydroxylation	250.1437	2.19E+08	3.17E+08	9.14E+05	1.87E+06
M3	Dihydroxylation	266.1386	4.45E+06	4.84E+07	-	-
M4	Dihydroxylation	266.1386	5.51E+07	4.59E+07	-	-
M5	Dihydroxylation	266.1386	5.61E+07	2.12E+08	-	-
M6	Dihydroxylation	266.1386	1.19E+06	1.97E+07	-	-
M7	Trihydroxylation	282.1335	9.13E+06	-	-	-
M8	Carboxylation	264.1230	1.32E+07	1.30E+08	-	-
M9	Hydroxylation + *O*-glucuronidation	426.1758	7.09E+06	-	-	-
M10	*N*-acetylation	276.1593	1.91E+07	7.17E+05	1.52E+07	8.40E+07
M11	*N*-acetylation + hydroxylation	292.1543	6.20E+07	-	-	-
M12	*N*-acetylation + dihydroxylation	308.1492	4.37E+06	-	-	-
2C-EF-FLY	Parent compound	252.1394	7.62E+07	1.00E+09	6.23E+08	1.38E+09
M1	Oxidative defluorination	250.1437	1.65E+07	6.68E+07	-	-
M14	Hydroxylation	268.1343	-	1.11E+08	-	-
M15	Hydroxylation	268.1343	1.78E+08	5.41E+08	-	-
M16	Dihydroxylation	284.1292	2.72E+07	6.39E+07		
M17	Dihydroxylation	284.1292	5.93E+06	2.32E+07	-	-
M8	Oxidative defluorination + oxidation to carboxylic acid	264.1230	1.54E+07	6.11E+07	-	-
M18	*N*-acetylation	294.1499	1.03E+07	7.00E+05	3.52E+06	4.29E+07
2C-T-7-FLY	Parent compound	280.1365	5.19E+07	5.23E+08	5.54E+08	5.15E+08
M20	Oxidation to sulfoxide	296.1314	3.12E+07	2.98E+08	7.16E+05	1.96E+06
M21	Hydroxylation	296.1314	6.24E+07	7.12E+08	7.37E+05	2.11E+06
M22	Oxidation to sulfone	312.1263	7.46E+06	8.29E+07	-	-
M23	Dihydroxylation	312.1263	-	1.41E+07	-	-
M24	Carboxylation	310.1107	2.63E+07	1.98E+08	-	-
M25	*S*-Dealkylation	238.0895	-	-	-	-
M26	*N*-acetylation	322.1471	-	8.59E+05	1.19E+07	4.01E+07
M27	*N*-acetylation + oxidation to sulfoxide	338.1420	1.71E+08	1.68E+07	9.08E+04	2.28E+06
M28	*N*-acetylation + oxidation to sulfone	354.1369	1.31E+09	7.29E+07	-	-
M29	*N*-acetylation + carboxylation	352.1212	2.58E+08	1.11E+07	-	-

fragmentation patterns in their MS^2 spectra were interpreted and compared to those of the parent compounds. Analytical information of the parent compounds and all phase I and II metabolites are listed in Tables 1 and 2. The given masses are the calculated exact masses. In total, the analyses of rat urine and in vitro incubations resulted in detections of several tentative metabolites: 2C-E-FLY, 13 metabolites; 2C-EF-FLY, 8 metabolites; and 2C-T-7-FLY, 11 metabolites. The resulting metabolic pathways can be found in Figures 2–4.

Fragmentation patterns of 2C-E-FLY and its metabolites are discussed exemplarily in the following as data of 2C-EF-FLY, 2C-T-7-FLY, and their metabolites were comparable. The MS^2 spectrum of the parent compound 2C-E-FLY ($M + H^+$, PM at m/z 234.1488, $C_{14}H_{20}O_2N$) showed an initial loss of ammonia (−17 u, NH_3, fragment ion, FI at m/z 217.1222, $C_{14}H_{17}O_2$). Afterwards, an ethyl moiety was eliminated (−29 u, C_2H_5, FI at m/z 188.0831, $C_{12}H_{12}O_2$). The FI at m/z 161.0596 ($C_{10}H_9O_2$) represented the intact 2,3,6,7-tetrahydrobenzo[1,2-b:4,5-b']difuran core before cleavage of one of the tetrahydrofuran rings with only a methyl group remaining at the benzene ring (FI at m/z 133.0647, C_9H_9O). The hydroxy metabolites (M1 and 2) also showed the loss of ammonia (FI at m/z 233.1171, $C_{14}H_{17}O_3$) and afterwards an elimination of water (−18 u, H_2O) resulting in a shift of 2 u from FI at m/z 217.1222 (2C-E-FLY) to 215.1066 (M1 and 2, $C_{14}H_{15}O_2$). For M1, the position of the hydroxy group was considered outside the 2,3,6,7-tetrahydrobenzo[1,2-b:4,5-b']difuran core. The double bond at the ethyl moiety formed after loss of water was afterwards eliminated resulting in the two FI at m/z 190.0988 ($C_{12}H_{14}O_2$) and 175.0753 ($C_{11}H_{11}O_2$) representing an unchanged 2,3,6,7-tetrahydrobenzo[1,2-b:4,5-b']difuran core with a remaining ethyl and methyl moiety, respectively. It is likely, that the hydroxy group was located at the terminal carbon atom of the ethyl moiety because the corresponding carboxy metabolite (M8) was also identified. In contrast to M1, M2 was probably hydroxylated at the 2,3,6,7-tetrahydrobenzo[1,2-b:4,5-b']difuran core due to the FI at m/z 131.0491 (C_9H_7O), which had an additional double bond in comparison to the FI at m/z 133.0647 (2C-E-FLY). The FI at m/z 215.1066 ($C_{14}H_{15}O_2$), 187.1117 ($C_{13}H_{15}O$), and 159.0804 ($C_{11}H_{11}O$) also provided a double bond inside of the ring system. However, exact positions of the hydroxy groups could not be identified based on fragmentation patterns.

Four dihydroxy metabolites (M3–M6) could be identified. For M3, the hydroxy groups were located at the ethyl moiety and the ethyl amine part as confirmed by the FI 175.0753 ($C_{11}H_{11}O_2$) with an unchanged 2,3,6,7-tetrahydrobenzo[1,2-b:4,5-b']difuran core. M4 and M5 most probably had one of their hydroxy groups at the 2,3,6,7-tetrahydrobenzo[1,2-b:4,5-b']difuran core due to the FI at m/z 131.0491 in accordance to M2. M5 was thought to also contain a hydroxy group at the ethyl moiety and represented therefore a combination of M1 and M2. In the case of M6, both hydroxylations are

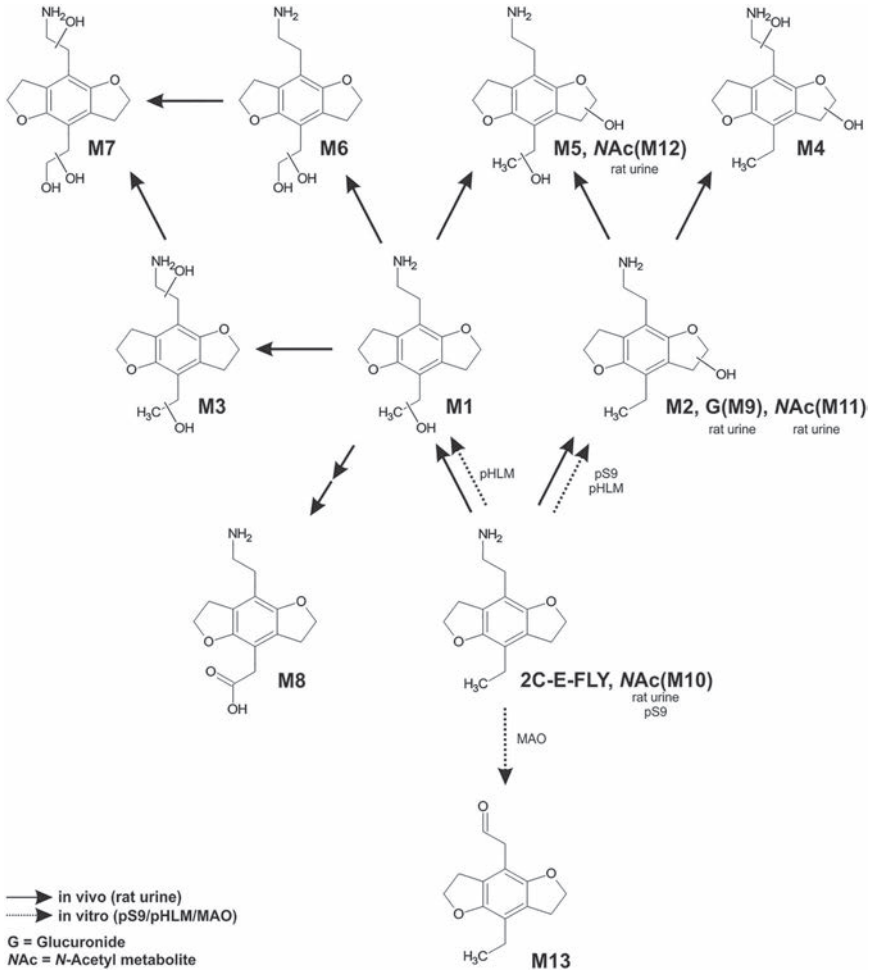

FIGURE 2 Metabolic pathways of 2C-E-FLY detected in rat urine or in in vitro incubations with pooled human liver S9 fraction (pS9), pooled human liver microsomes (pHLMs), or recombinant human monoamine oxidases (MAOs)

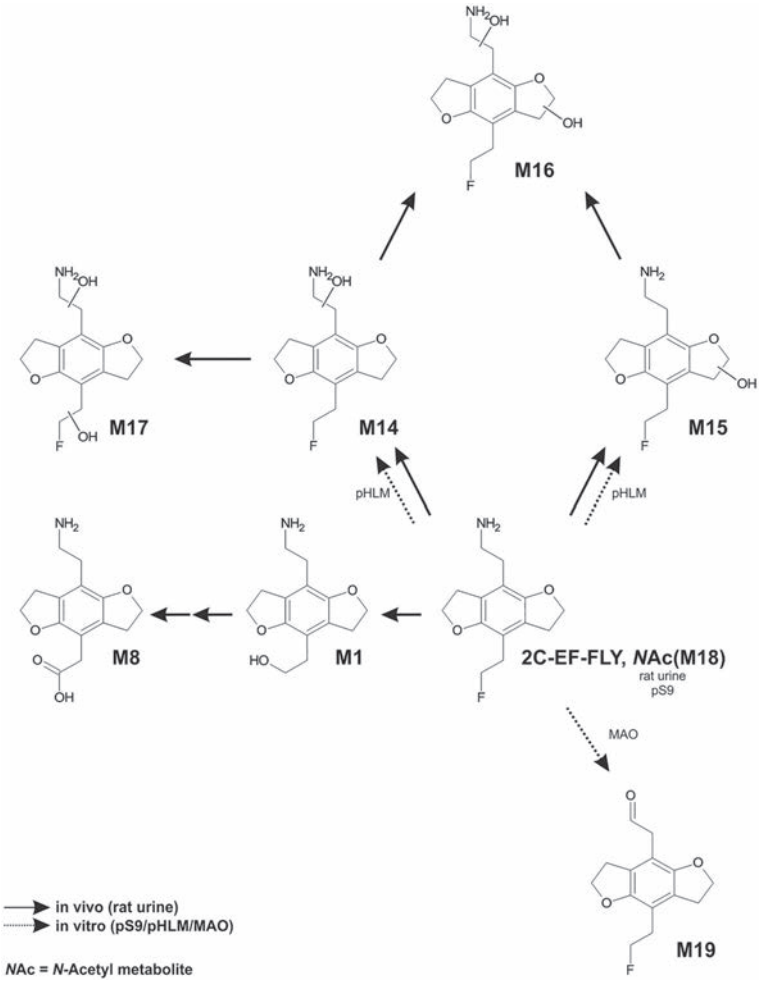

FIGURE 3 Metabolic pathways of 2C-EF-FLY detected in rat urine or in in vitro incubations with pooled human liver S9 fraction (pS9), pooled human liver microsomes (pHLMs), or recombinant human monoamine oxidases (MAOs)

determined to be located at the ethyl moiety. Again, initial steps were loss of ammonia and water, followed by the elimination of CO (−28 u from the FI at m/z 231.1015 ($C_{14}H_{15}O_3$) leading to the FI at m/z 203.1066 ($C_{13}H_{15}O_2$). Furthermore, the presence of FI at m/z 175.0753 ($C_{11}H_{11}O_2$) indicated an unchanged 2,3,6,7-tetrahydrobenzo[1,2-b:4,5-b']difuran core. One trihydroxy metabolite (M7) could also be identified. The absence of a hydroxy group at the 2,3,6,7-tetrahydrobenzo[1,2-b:4,5-b']difuran core was confirmed by the FI at m/z 175.0753 ($C_{11}H_{11}O_2$). According to Niessen et al, the carboxylic acid, such as that one found in the carboxy metabolite (M8), can be eliminated in two steps.[25] After initial loss of the ammonia (FI at m/z 247.0964, $C_{14}H_{15}O_4$), the elimination of water (−18 u, H_2O) led to the FI at m/z 229.0858 ($C_{14}H_{13}O_3$) followed by a rearrangement of the double bonds resulting in the formation of an oxonium ion. Subsequently, CO was eliminated and led to the FI at m/z 201.0909 ($C_{13}H_{13}O_2$). It should be considered, that M1 and M8 can also be formed during metabolic transformation of 2C-EF-FLY after oxidative defluorination. In conclusion, both metabolites are not suitable for unambiguous identification of an intake of 2C-E-FLY or 2C-EF-FLY and could lead to an incorrect interpretation of analytical findings.

Concerning phase II metabolites of 2C-E-FLY, one *O*-glucuronide and three *N*-acetylated metabolites could be detected (M9–M12). The fragmentation pattern of the *O*-glucuronide (M9, PM at m/z 426.1758, $C_{20}H_{28}O_9N$) was in accordance to the corresponding phase I metabolite (M2) after elimination of glucuronic acid (−176 u, $C_6H_8O_6$). After elimination of the acetyl moiety (−42 u, C_2H_2O), the *N*-acetyl metabolite (M10, PM at m/z 276.1593, $C_{16}H_{22}O_3N$) provided the same fragmentation pattern as 2C-E-FLY. M2 and M5 were also found to be N-acetylated in vivo (M11 + 12). In comparison to the corresponding phase I metabolites, M11 and M12 provided additional FI in their MS^2 spectrum (M11 at m/z 274.1437, $C_{16}H_{20}O_3N$, and M12 at m/z 290.1386, $C_{16}H_{20}O_4N$, and m/z 272.1280, $C_{14}H_{20}O_3N$) formed after elimination of water (−18 u, H_2O) before elimination of the acetyl moiety.

In summary, most metabolites were detected in rat urine after precipitation and only few metabolites were formed in incubations with pS9 fraction. This was most probably caused by the different experimental conditions. First of all, pS9 incubations were stopped after a maximum of 6 hours, while rat urine was collected over a 24-hour period. In addition, in vitro experiments have limitations concerning distribution and excretion leading to simple metabolites formed after few reaction steps. Last but not least, species differences can be followed by formation of different metabolites. However, to conclude which model is most suitable for developing urine screening approaches, authentic human urine would be needed. An intake by humans in the framework of a controlled trial would be the gold standard, but is

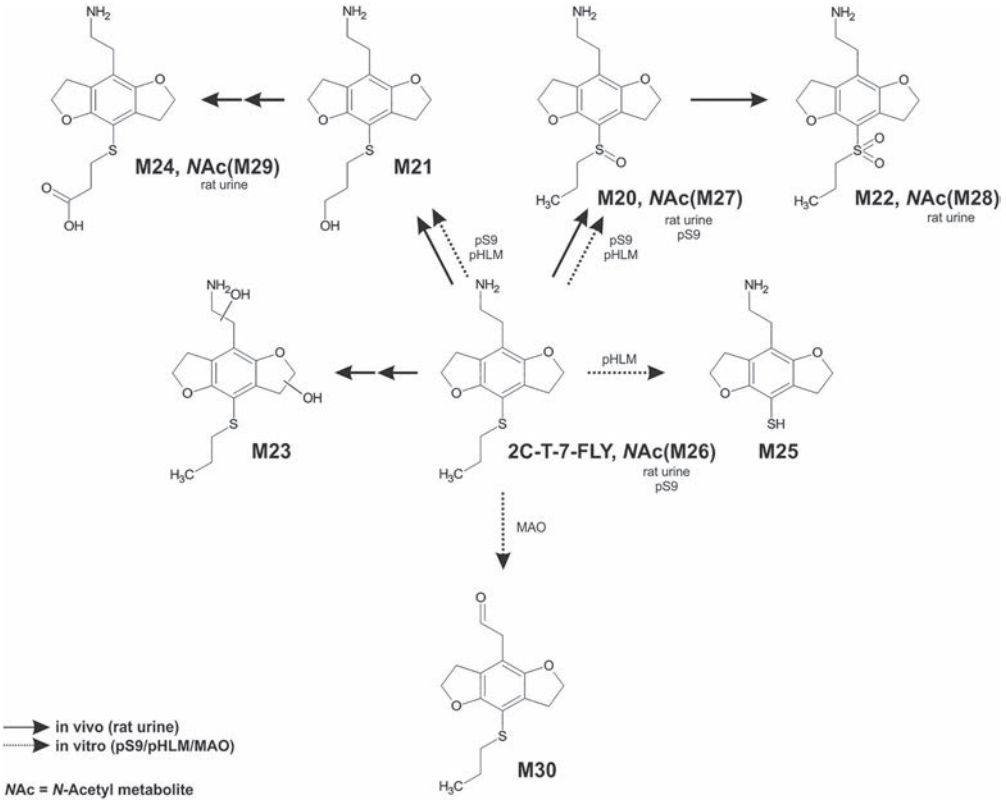

FIGURE 4 Metabolic pathways of 2C-T-7-FLY detected in rat urine or in in vitro incubations with pooled human liver S9 fraction (pS9), pooled human liver microsomes (pHLMs), or recombinant human monoamine oxidases (MAOs)

TABLE 3 General involvement of tested cytochrome P450 (CYP) isoenzymes and flavin-containing monooxygenase 3 (FMO3) in metabolic phase I steps. -, not detected

Metabolic step	2C-E-FLY	2C-EF-FLY	2C-T-7-FLY
Hydroxylation (chain)	CYP2D6 CYP3A4	CYP2D6	CYP2D6
Hydroxylation (core)	CYP2D6	CYP2D6	-
Oxidation to sulfoxide	-	-	CYP3A4 FMO3
S-Dealkylation	-	-	CYP2D6 CYP3A4

TABLE 4 Toxicological detectability of 2C-E-FLY, 2C-EF-FLY, and 2C-T-7-FLY in rat urine by the GC–MS standard urine screening approach. BW, body weight; +, detected; −, not detected; AC, acetylated

Compound	Precursor Ion Mass, *m/z*	Elemental Composition	Retention Index (RI)	Characteristic Fragment Ions, *m/z*	Administered Dose, mg/kg BW	
					0.2	2
2C-E-FLY-M (hydroxy) -H_2O AC	273	$C_{16}H_{19}O_3N$	2320	199, 214	−	+
2C-EF-FLY AC	293	$C_{16}H_{20}O_3NF$	2480	221, 234	+	+
2C-EF-FLY-M (hydroxy) -H_2O AC	291	$C_{16}H_{18}O_3NF$	2450	199, 219, 232	+	+
2C-EF-FLY-M (dihydroxy) -2H_2O AC	289	$C_{16}H_{16}O_3NF$	2420	197, 217, 230	+	+
2C-T-7-FLY AC	321	$C_{17}H_{23}O_3NS$	2720	207, 219, 249, 262	−	+
2C-T-7-FLY-M (hydroxy) -H_2O AC	319	$C_{17}H_{21}O_3NS$	2690	205, 247, 260	−	+
2C-T-7-FLY-M (hydroxy) 2 AC	379	$C_{19}H_{25}O_5NS$	2890	101, 218, 260, 320	−	+
2C-T-7-FLY-M (dihydroxy) -H_2O 2 AC	377	$C_{19}H_{23}O_5NS$	2850	101, 216, 258, 318	−	+

considered as unethical, time consuming, and expensive.[26] Nevertheless, human biosamples after intake of NPS derived from authentic cases are sometimes available and should then be used for a comparative study summarizing all metabolites detected in vitro and in vivo.

3.2 | Investigation of isoenzyme activities

3.2.1 | Monooxygenases activity screening

The monooxygenases activity screening was performed to investigate the impact of ten CYP isoenzymes and FMO3 on phase I metabolism of the three 2C-FLY derivatives. Incubations with pHLM were used as positive control. Results are summarized in Table 3. The side chain hydroxylation of 2C-EF-FLY and 2C-T-7-FLY was catalyzed by CYP2D6 and additionally by CYP3A4 in case of 2C-E-FLY. Hydroxylation of the 2,3,6,7-tetrahydrobenzo[1,2-b:4,5-b']difuran core of 2C-E-FLY and 2C-EF-FLY was catalyzed by CYP2D6. The thioether moiety of 2C-T-7-FLY was oxidized to the sulfoxide (M20) by CYP3A4 and FMO3. *S*-Dealkylation of 2C-T-7-FLY (M25) was catalyzed by CYP2D6 and CYP3A4 and was detected neither in rat urine nor in pS9 incubations.

3.2.2 | Monoamine oxidases activity screening

Due to the primary amine contained in the structure of the 2C-FLY drugs, a deamination catalyzed by MAO isoforms was likely to occur and this metabolic step was already described for 2C compounds.[14,27] However, due to the loss of nitrogen, neither the detection of the deaminated metabolite nor the expected end-products (oxidized carboxylic acid or reduced alcohol) was possible with the used settings. Therefore, incubations with MAO-A or B and the aldehyde trapping agent methoxyamine were performed. The deaminated metabolites (M13, 19, 30) could afterwards be detected as oxime adducts of the 2C-FLY drugs and methoxyamine. For M13 (PM at m/z 262.1437, $C_{15}H_{20}O_3N$), the oxime moiety plus one carbon atom was eliminated resulting in FI at m/z 203.1066 ($C_{13}H_{15}O_2$) in the first fragmentation step. Afterwards, the ethyl moiety was eliminated in subsequent steps (FI at m/z 190.0988, $C_{12}H_{14}O_2$, and 175.0753, $C_{11}H_{11}O_2$). The deamination of all three 2C-FLY derivatives was found to be catalyzed by MAO-A and B. Further kinetic studies would allow to assess, which isoenzyme is the main catalyzing isoform.

3.2.3 | *N*-Acetyltransferases activity screening

N-Acetylation of the primary amines was found to be one of the main metabolic steps. In order to investigate which NAT isoenzyme catalyzed this reaction, a NAT activity screening was performed and both isoforms, NAT1 and NAT2, catalyzed the reaction. Again, further kinetic studies would allow assessment of which isoenzyme is the main catalyzing isoform.

3.3 | Toxicological detectability in rat urine

No information concerning dosage of 2C-E-FLY, 2C-EF-FLY, and 2C-T-7-FLY in humans could be found but oral 2C-B-FLY doses of 10–20 mg were described.[14] This was comparable to 2C-B dosages of 12–24 mg as recommended by Shulgin and Shulgin, who also listed dosages of 10–30 mg for 2C-E and 2C-T-7.[28] Rat doses of 0.2 (low dose) or 2 mg/kg BW (high dose) corresponded to human doses of 0.03 and 0.33 mg/kg BW, respectively,[29] which would be a human oral dose of 2 or 23 mg for a BW of 70 kg. Therefore, recreational doses should be

TABLE 5 Toxicological detectability of 2C-E-FLY, 2C-EF-FLY, and 2C-T-7-FLY in rat urine by the LC–IT–MS standard urine screening approach. Precursor ions of the MS^3 fragment ions are given in brackets. Metabolite iDs correspond to Table 1. BW, body weight; D, precursor ion in MS^1 detected; I, identified due to MS^2 spectrum

Metabolite iD	Parent Compound or Metabolite	Precursor Ion Mass, m/z	Retention Time, Min	Characteristic MS^2 Fragment Ions at m/z	Characteristic MS^3 Fragment Ions at m/z	Administered Dose, mg/kg BW	
						0.2	2
Parent compound	**2C-E-FLY**	234	10.38	217, 189, 188, 171, 161	(189) 161, 133	D	I
M1	**2C-E-FLY-M** (hydroxy)	250	5.94	215, 190, 189, 162	(190) 162, 147, 133	D	I
M2	**2C-E-FLY-M** (hydroxy)	250	6.70	215, 203, 187, 159	(215) 187, 159	I	I
M4	**2C-E-FLY-M** (dihydroxy)	266	4.90	231, 230, 219, 201	(230) 201	D	I
M5	**2C-E-FLY-M** (dihydroxy)	266	5.76	231, 230, 213	(230) 202, 185, 147	D	I
M10	**2C-E-FLY-M** (N-acetyl)	276	15.32	240, 234, 220, 176, 142, 129	(220) 142, 129	I	I
M11	**2C-E-FLY-M** (N-acetyl hydroxy)	292	8.49	250, 233, 232, 215	(215) 187, 186, 159	D	I
Parent compound	**2C-EF-FLY**	252	8.69	215, 207, 187, 159	(215) 159	I	I
M8	**2C-EF-FLY-M** (oxidative defluorination and oxidation)	264	7.45	229, 201, 187, 159, 109	(229) 201, 187	I	I
M21	**2C-T-7-FLY-M** (hydroxy)	296	7.57	261, 221, 189, 161, 149	(189) 161, 149	I	I
M28	**2C-T-7-FLY** (N-acetyl sulfone)	354	6.81	294, 247, 235, 188	(247) 188	I	I

TABLE 6 Toxicological detectability of 2C-E-FLY, 2C-EF-FLY, and 2C-T-7-FLY in rat urine by the LC-HRMS/MS standard urine screening approach. Metabolite iDs correspond to Table 1. BW, body weight; –, not detected; D, precursor ion in MS^1 detected; I, identified due to MS^2 spectrum

Metabolite iD	Parent Compound or Metabolite	Exact Precursor Ion Mass, *m/z*	Retention Time, Min	Administered Dose, mg/kg BW	
				0.2	2
Parent compound	2C-E-FLY	234.1488	6.20	D	I
M1	2C-E-FLY-M (hydroxy)	250.1437	4.95	D	I
M2	2C-E-FLY-M (hydroxy)	250.1437	5.29	I	I
M4	2C-E-FLY-M (dihydroxy)	266.1386	4.50	D	I
M5	2C-E-FLY-M (dihydroxy)	266.1386	4.77	D	I
M10	2C-E-FLY-M (*N*-acetyl)	276.1593	7.77	D	I
M11	2C-E-FLY-M (*N*-acetyl hydroxy)	292.1543	6.14	D	I
Parent compound	2C-EF-FLY	252.1394	5.80	I	I
M15	2C-EF-FLY-M (hydroxy)	268.1343	4.99	I	I
M8	2C-EF-FLY-M (carboxy)	264.1230	5.02	-	I
M18	2C-EF-FLY-M (*N*-acetyl)	294.1499	7.40	-	I
Parent compound	2C-T-7-FLY	280.1365	6.88	-	I
M20	2C-T-7-FLY-M (sulfoxide)	296.1314	5.37	I	I
M21	2C-T-7-FLY-M (hydroxy)	296.1314	5.55	D	I
M24	2C-T-7-FLY-M (carboxy)	310.1107	5.70	D	I
M27	2C-T-7-FLY-M (*N*-acetyl sulfoxide)	338.1420	6.69	I	I
M28	2C-T-7-FLY-M (*N*-acetyl dihydroxy)	354.1369	5.65	I	I
M29	2C-T-7-FLY-M (*N*-acetyl carboxy)	352.1213	6.89	I	I

expected to be in the range of the high dose, whereas doses resulting in severe intoxications are expected to be even higher.

3.3.1 | GC–MS SUSA

Results are summarized in Table 4. After low dose administration, only 2C-EF-FLY and two metabolites could be detected. The observed elimination of water is probably attributed to the high temperature in the injection port. After high dose administration, 2C-T-7-FLY and three of its metabolites could be detected and additionally one 2C-E-FLY metabolite. Based on these data, it could not be stated whether this metabolite was hydroxy 2C-E-FLY isomer 1 or 2 and therefore whether it was a substance-specific metabolite or not. Acetylation during sample preparation resulted in the sum of acetylated parent compound/metabolite and the corresponding, metabolically formed *N*-acetyl metabolite (M11, M18, M26, M27).

3.3.2 | LC–IT–MS SUSA

Results are summarized in Table 5. After low and high dose administration, the three 2C-FLY drugs and/or their metabolites could be identified in rat urine based on the corresponding MS^2 spectra. In conclusion, an intake should be detectable by the LC-IT-MS SUSA.

3.3.3 | LC–HRMS/MS SUSA

Results are summarized in Table 6. Similar to the LC–IT–MS SUSA, the three 2C-FLY drugs and/or their metabolites could be identified in rat urine after low and high dose administration by the corresponding MS^2 spectra. An intake is thus expected to be detectable by the LC–HRMS/MS SUSA.

4 | CONCLUSIONS

In total, 32 metabolites of 2C-E-FLY, 2C-EF-FLY, and 2C-T-7-FLY could be identified in rat urine and in vitro incubations. Hydroxylation and *N*-acetylation were identified as main metabolic steps, whereas methoxyamine was successfully used for detection of the deaminated metabolites formed by MAO-A and B. Most metabolites were identified in rat urine after precipitation. Phase I metabolic reactions were mainly catalyzed by CYP2D6 and CYP3A4 and *N*-acetylation by NAT1 and NAT2. Intoxications with these NPS should be detectable by all three tested SUSAs, but common metabolites of 2C-E-FLY and 2C-EF-FLY (M1, M8) have to be considered during interpretation of analytical findings.

ACKNOWLEDGEMENTS

The authors would like to thank Gabriele Ulrich, Hans H. Maurer, and Armin A. Weber for their support.

CONFLICT OF INTEREST

The authors declare that there are no conflicts of interest.

ORCID

Simon D. Brandt https://orcid.org/0000-0001-8632-5372
Markus R. Meyer https://orcid.org/0000-0003-4377-6784

REFERENCES

1. World Drug Report 2018. UNODC; 2018. https://www.unodc.org/wdr2018/index.html. Accessed 10/07/2018.
2. EMCDDA. European drug report 2018. Publications of the European Union. 2018. http://www.emcdda.europa.eu/system/files/publications/8585/20181816_TDAT18001ENN_PDF.pdf.
3. Rojek S, Klys M, Maciow-Glab M, Kula K, Strona M. Cathinones derivatives-related deaths as exemplified by two fatal cases involving methcathinone with 4-methylmethcathinone and 4-methylethcathinone. *Drug Test Anal*. 2014;6(7-8):770-777.
4. Caspar AT, Helfer AG, Michely JA, et al. Studies on the metabolism and toxicological detection of the new psychoactive designer drug 2-(4-iodo-2,5-dimethoxyphenyl)-N-[(2-methoxyphenyl)methyl]ethanamine (25I-NBOMe) in human and rat urine using GC-MS, LC-MS(n), and LC-HR-MS/MS. *Anal Bioanal Chem*. 2015;407(22):6697-6719.
5. Abouchedid R, Ho JH, Hudson S, et al. Acute toxicity associated with use of 5F-derivations of synthetic cannabinoid receptor agonists with analytical confirmation. *J Med Toxicol*. 2016;12(4):396-401.
6. Adamowicz P, Tokarczyk B, Stanaszek R, Slopianka M. Fatal mephedrone intoxication--a case report. *J Anal Toxicol*. 2013;37(1):37-42.
7. Andreasen MF, Telving R, Birkler RI, Schumacher B, Johannsen M. A fatal poisoning involving Bromo-dragonfly. *Forensic Sci Int*. 2009;183(1–3):91-96.
8. Meyer MR, Maurer HH. Metabolism of designer drugs of abuse: an updated review. *Curr Drug Metab*. 2010;11(5):468-482.
9. Halberstadt AL, Chatha M, Stratford A, Grill M, Brandt SD. Comparison of the behavioral responses induced by phenylalkylamine hallucinogens and their tetrahydrobenzodifuran ("FLY") and benzodifuran ("Dragon-FLY") analogs. *Neuropharmacology*. 2019;144:368-376.
10. Monte AP, Marona-Lewicka D, Parker MA, Wainscott DB, Nelson DL, Nichols DE. Dihydrobenzofuran analogues of hallucinogens. 3. Models of 4-substituted (2,5-dimethoxyphenyl)alkylamine derivatives with rigidified methoxy groups. *J Med Chem*. 1996;39(15):2953-2961.
11. Rickli A, Kopf S, Hoener MC, Liechti ME. Pharmacological profile of novel psychoactive benzofurans. *Br J Pharmacol*. 2015;172(13):3412-3425.
12. King LA. New phenethylamines in Europe. *Drug Test Anal*. 2014;6(7–8):808-818.
13. Wagmann L, Brandt SD, Stratford A, Maurer HH, Meyer MR. Interactions of phenethylamine-derived psychoactive substances of the 2C-series with human monoamine oxidases. *Drug Test Anal*. 2019;11(2):318-324.
14. Noble C, Holm NB, Mardal M, Linnet K. Bromo-dragonfly, a psychoactive benzodifuran, is resistant to hepatic metabolism and potently inhibits monoamine oxidase a. *Toxicol Lett*. 2018;295:397-407.
15. Wagmann L, Richter LHJ, Kehl T, et al. In vitro metabolic fate of nine LSD-based new psychoactive substances and their analytical detectability in different urinary screening procedures. *Anal Bioanal Chem*. 2019;411(19):4751-4763.
16. Caspar AT, Westphal F, Meyer MR, Maurer HH. LC-high resolution-MS/MS for identification of 69 metabolites of the new psychoactive substance 1-(4-ethylphenyl-)-N-[(2-methoxyphenyl)methyl] propane-2-amine (4-EA-NBOMe) in rat urine and human liver S9 incubates and comparison of its screening power with further MS techniques. *Anal Bioanal Chem*. 2018;410(3):897-912.
17. Richter LHJ, Maurer HH, Meyer MR. Metabolic fate of the new synthetic cannabinoid 7'N-5F-ADB in rat, human, and pooled human S9 studied by means of hyphenated high-resolution mass spectrometry. *Drug Test Anal*. 2019;11(2):305-317.
18. Wissenbach DK, Meyer MR, Remane D, Philipp AA, Weber AA, Maurer HH. Drugs of abuse screening in urine as part of a metabolite-based LC-MSn screening concept. *Anal Bioanal Chem*. 2011;400(10):3481-3489.
19. Maurer HH, Pfleger K, Weber AA. *Mass spectral data of drugs, poisons, pesticides, pollutants and their metabolites*. Weinheim: Wiley-VCH; 2016.
20. Richter LHJ, Maurer HH, Meyer MR. New psychoactive substances: studies on the metabolism of XLR-11, AB-PINACA, FUB-PB-22, 4-methoxy-alpha-PVP, 25-I-NBOMe, and meclonazepam using human liver preparations in comparison to primary human hepatocytes, and human urine. *Toxicol Lett*. 2017;280:142-150.
21. Wagmann L, Meyer MR, Maurer HH. What is the contribution of human FMO3 in the N-oxygenation of selected therapeutic drugs and drugs of abuse? *Toxicol Lett*. 2016;258:55-70.
22. Meyer MR, Lindauer C, Maurer HH. Dimethocaine, a synthetic cocaine derivative: studies on its in vitro metabolism catalyzed by P450s and NAT2. *Toxicol Lett*. 2014;225(1):139-146.
23. Meyer MR, Robert A, Maurer HH. Toxicokinetics of novel psychoactive substances: characterization of N-acetyltransferase (NAT) isoenzymes involved in the phase II metabolism of 2C designer drugs. *Toxicol Lett*. 2014;227(2):124-128.
24. Helfer AG, Michely JA, Weber AA, Meyer MR, Maurer HH. Orbitrap technology for comprehensive metabolite-based liquid chromatographic-high resolution-tandem mass spectrometric urine drug screening - exemplified for cardiovascular drugs. *Anal Chim Acta*. 2015;891:221-233.
25. Niessen WM, Correa RA. *Interpretation of MS-MS Mass Spectra of Drugs and Pesticides*. Hoboken, New Jersey: John Wiley & Sons; 2016.
26. Wagmann L, Manier SK, Eckstein N, Maurer HH, Meyer MR. Toxicokinetic studies of the four new psychoactive substances 4-chloroethcathinone, N-ethylnorpentylone, N-ethylhexedrone, and 4-fluoro-alpha-pyrrolidinohexiophenone. *Forensic Toxicol*. 2019:1-11. in press. https://doi.org/10.1007/s11419-019-00487-w
27. Theobald DS, Maurer HH. Identification of monoamine oxidase and cytochrome P450 isoenzymes involved in the deamination of phenethylamine-derived designer drugs (2C-series). *Biochem Pharmacol*. 2007;73(2):287-297.
28. Shulgin A, Shulgin A. *Pihkal, a chemical love story*. Berkley (CA): Transform Press; 1991.
29. Sharma V, McNeill JH. To scale or not to scale: the principles of dose extrapolation. *Br J Pharmacol*. 2009;157(6):907-921.

How to cite this article: Wagmann L, Hempel N, Richter LHJ, Brandt SD, Stratford A, Meyer MR. Phenethylamine-derived new psychoactive substances 2C-E-FLY, 2C-EF-FLY, and 2C-T-7-FLY: Investigations on their metabolic fate including isoenzyme activities and their toxicological detectability in urine screenings. *Drug Test Anal*. 2019;11:1507-1521. https://doi.org/10.1002/dta.2675